# Localized surface plasmon resonance of nanotriangle dimers at different relative positions

Yatao Ren, Hong Qi*, Qin Chen, Shenling Wang, Liming Ruan*

*School of Energy Science and Engineering, Harbin Institute of Technology, 92, West Dazhi Street, Harbin, Heilongjiang, 150001, PR China*

## ARTICLE INFO

## ABSTRACT

The investigation of nanoparticle's optical properties is crucial for their biological and therapeutic applications. In the present work, a promising type of gold nanoparticle, the triangular prism which was reported to have multipolar surface plasmon peaks, was studied. The Plasmon ruler effect of nanotriangle dimers was observed and investigated for the first time. Well-defined trends of the extinction spectra maxima, which have a linear correlation with the triangle edge length, for lower order extinction corresponding to in-plane mode, were observed. On this basis, the optical property of nanotriangle dimers with different arrangements, including two nanotriangles aligned side-by-side, bottom-to-bottom, and in line, were studied. For the side-by-side arrangement, an additional peak was generated on the red shift side of the peak corresponding to dipole mode. When the distance between two prisms was scaled by the triangular side length, the relative plasmon shift can be approximated as an exponential function of the relative offset distance. Moreover, for dimers with nanotriangles arranged in line, there was a global blue shift of the extinction spectra with the approaching of two particles, including the higher order mode extinction. An interesting phenomenon was found for dimers with two nanotriangles aligned bottom-to-bottom. The resonance band split into two bands with the decreasing of the offset distance.

© 2017 Elsevier Ltd. All rights reserved.

## 1. Introduction

With rapid growth of nanotechnology being applied in various fields, such as medicine/pharmacology [1-4], energy harvesting [5,6], and biology [7-9], researches that focus on the synthesis and evaluation of nanomaterial are attracting more and more attentions [9-12]. Due to the superior optical, biological, and chemical properties, noble metal nanoparticles with various morphologies, such as nanosphere, nanorod, nanoshell, nanocage, nanostar etc., are often employed as contrast agent [13,14] and drug carrier [15]. For example, the laser induced thermal therapy (LITT) usually takes advantage of the thermal response which is generated by the interaction between laser and injected nanoparticles, also known as surface plasmon resonance (SPR). The quantification of thermal effect is strongly dependent on the optical properties, i.e. absorption and scattering, of the nanoparticles. Furthermore, in the 'optical window' region, the tissue has a relative low absorption, which allows the light to propagate through a long distance and also weakens the local heating phenomenon for the healthy tissue [16]. The selective heat requires that the cancerous tissue has a relatively high absorption compared with surrounding healthy tissue. Therefore, the peak in the absorption spectra is an extremely important parameter that needs to be fully investigated. The optical properties of nanoparticle vary with the size, shape, composition, and properties of surrounding materials [17,18]. As mentioned above, though there are quite a few different shapes of nanoparticles being investigated, the optical properties of those nanoparticles and influence factors still need to be fully addressed.

Interesting optical properties of nanotriangles are illustrated owing to its high aspect ratio [19], which makes nanotriangle a promising candidate for nanomedicine and other related areas. The nanotriangle prisms have multipolar plasmon extinction effect, which is generated by localized surface plasmon and lighting rod effects [20]. These effects have been thoroughly studied numerically and experimentally for nanotriangles and other morphologis [20-24]. The single peak in visible region for small particles corresponds to the dipole mode. With the increasing of the particle radius, the peaks generated by higher order resonance become important [21]. Also, size, shape, and other geometric parameters has significant influence on thermal and optical performance of nanoparticles or nanostructures [25], which needs to be investigated thoroughly. Nanotriangle has a very broad SPR band in the near-infrared, which is an outstanding properties for photothermal therapy and other applications. The interaction between two nanoparticles are of great importance [26,27]. Therefore, in recent

year, efforts have been made to investigate the plasmon coupling of nanotriangle dimers. The influence factors for optical properties of nanotriangle dimers with different types have been investigated, including the gap distance, coating thickness, nanotriangle thickness, and different coupling types [28-33]. It is found that there will be a redshift of the resonance wavelength when the thickness and gap width of bowtie nanotriangle decreases [28]. Furthermore, for the edge-to-edge nanotriangle dimer, two separated Plasmon modes are observed and can be tuned by changing the misalign distance [31]. However, previous studies mainly deal with the optical properties of nanotriangle dimers qualitatively. Herein, we present some quantitative results of exactly how the gap between different types of nanotriangle dimers influences their spectral characteristics, which are important to the precise control of optical response in their applications.

To calculate the absorption and scattering properties of particles, the Maxwell's equations need to be solved. The analytical solution can be obtained by Mie theory [34]. However, it is only suitable for homogeneous and isotropic spheres or spheroids. The discrete dipole approximation (DDA) method is one of the most versatile, important and widespread numerical methods to obtain the optical properties of small particles with arbitrary shapes and compositions, which also extended to the application of near-field recently [35,36]. The basic principle of DDA is to discretize a small particle into a cubic array of virtual $N$-point dipoles [37]. Then the scattering field of the whole particle can be approximated as the summation of all the dipoles. Theoretically speaking, DDA can be applied to calculate the optical properties of arbitrary shape target theoretically if it is properly discretized.

The interaction between two close nanoparticles will affect the localized SPR [26], which can be exploited in many applications, such as surface-enhanced Raman spectroscopy [38,39], universal plasmon ruler [40], nearfield image [41,42], and subwavelength optoelectronic devices [43,44]. It is worth to mention that the plasmon ruler effect has been applied to measure the distance between two metal nanoparticles in biological system [45,46] and optoelectronics [43,47], which usually concentrates on the usage of nanospheres. In 2009, Funston et al. studied the plasmon ruler effect of nanorod dimers [26]. However, the plasmon ruler effect of nanotriangles has not yet been observed and investigated. Therefore, in our present work, this effect is studied thoroughly, which is important to widen the application fields of plasmon ruler effect.

In the present work, the optical properties of gold nanotriangle dimers were studied. The size of nanotriangle can be changed to tune the absorption maximum to desired spectral region just like nanorod. Therefore, firstly, the influence of edge length was investigated. Afterwards, the optical properties for different types of nanotriangle dimers, including two nanotriangles aligned side-by-side, bottom-to-bottom, and in line, were studied. The influence of offset distance is found to have paramount influence on the performance of nanotriangle dimers. Also, multipolar surface plasmon peaks were observed duo to the interaction between two particles.

## 2. Theory and methods

The DDA method can be applied to calculate the optical properties of particles with arbitrary geometries and compositions. The DDA package, developed by Draine and Flatau [48], has been widely employed to calculate scattering and absorption of light by irregular particles. The basic principle of DDA is to discretize the target of interest into a cubic array of virtual $N$-point dipoles [37]. The polarization of the $i$th dipole is $\mathbf{P}_j = a_j\mathbf{E}_j$, where $\alpha_j$ is the polarizability of the $j$th dipole and $\mathbf{E}_j$ is the electric field in position $\mathbf{r}_j$, which can be expressed as:

$$\mathbf{E}_j = \mathbf{E}_j^{\text{inc}} - \sum_{k \neq j} \mathbf{A}_{jk}\mathbf{P}_k \tag{1}$$

where $\mathbf{E}_j^{\text{inc}}$ is the incident electric field, which is given by $\mathbf{E}_j^{\text{inc}} = \mathbf{E}_0 \exp(ik \cdot \mathbf{r}_j - i\omega t)$, where $\mathbf{E}_0$ is the amplitude of the electric field intensity and $k$ can be expressed as $\omega/c$. $\mathbf{A}_{jk}$ stands for the interaction matrix, where $j$ and $k$ is the number of dipoles. $\mathbf{A}_{jk}\mathbf{P}_k$ is the electric field at position $\mathbf{r}_j$, which is triggered by the dipole at position $\mathbf{r}_k$. It is given as [49]:

$$\mathbf{A}_{jk}\mathbf{P}_k = \frac{\exp\left(ik\mathbf{r}_{jk}\right)}{\mathbf{r}_{jk}^3}\left\{ k^2\mathbf{r}_{jk} \times \left(\mathbf{r}_{jk} \times \mathbf{P}_k\right) + \frac{\left(1 - ik\mathbf{r}_{jk}\right)}{\mathbf{r}_{jk}^2} \right.$$
$$\left. \times \left[\mathbf{r}_{jk}^2\mathbf{P}_k - 3\mathbf{r}_{jk} \cdot \mathbf{P}_k\right] \right\}, \quad j \neq k \tag{2}$$

If $\mathbf{A}_{jj}$ is defined as $\mathbf{A}_{jj} = -\alpha_j^{-1}$, then the scattering problem can be described as a set of linear equations as follows:

$$\sum_{k=1}^{N} \mathbf{A}_{jk}\mathbf{P}_k = \mathbf{E}_j^{\text{inc}} \tag{3}$$

The extinction, absorption, and scattering cross section can be calculated by:

$$C_{\text{ext}} = \frac{4\pi k}{|\mathbf{E}_0|^2} \sum_{j=1}^{N} \text{Im}\left(\mathbf{E}_j^{\text{inc},*} \cdot \mathbf{P}_j\right) \tag{4}$$

$$C_{\text{abs}} = \frac{4\pi k}{|\mathbf{E}_0|^2} \sum_{j=1}^{N} \left[\text{Im}\left(\mathbf{P}_j \cdot \alpha_j^{-1} \cdot \mathbf{P}_j^*\right) - \frac{2}{3}k^3\left|\mathbf{P}_j\right|^2\right] \tag{5}$$

$$C_{\text{sca}} = C_{\text{ext}} - C_{\text{abs}} \tag{6}$$

where $\mathbf{P}^*$ is the polarization of each dipole. The corresponding extinction, absorption, and scattering efficiency is the ratio of cross section and $\pi R_{\text{eff}}^2$, where $R_{\text{eff}}$ is the effective radius. $R_{\text{eff}}$ is invariably utilized to characterize the size of an arbitrary shape small particle, which can be expressed as $R_{eff} = (3V/4p)^{1/3}$, where $V$ is the volume of the particle.

The detailed description and mathematical formulation of DDA can be found elsewhere [48-50]. The results of DDA are compared with previous work [37,51], which is shown in Fig. 1. For the results of gold nanorod, the direction of electric field is parallel to the long axis. The dielectric constants of gold nanoparticles are
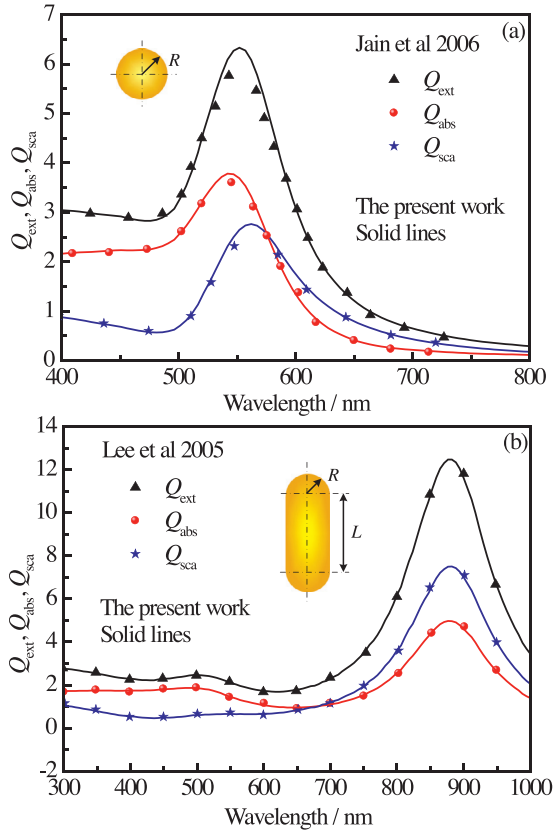
**Fig. 1.** Calculated spectra of extinction, absorption, and scattering efficiency for (a) nanosphere with $R = 40$ nm and (b) nanorod with $R_{eff} = 40$ nm and $L/2R = 2$.

regarded as the same as bulk metal [52]. The refractive index of the surrounding media is set as 1.33 and 1.34 for nanosphere and nanorod respectively, which is similar to water. It can be seen that the present results fitted well with previous work (see Fig. 1), which proves the validation of the present model. Furthermore, previous work has been done which utilizes DDA method to investigate the optical properties of triangular prism and nanoparticle dimers [26,31]. Therefore, for simplicity's sake, the validation of DDA for other shape will not be shown in the present work.

## 3. Results and discussion

For large and thin prisms, the extinction efficiency, where the polarization vector **E** of incident electromagnetic wave is parallel to the triangular cross section, is the most paramount [21], which can be seen in Fig. 2. Also it is obvious that the extinction spectra for different incident angles have the same trends. The only difference is the absolute value. Therefore, one of the three incident angles can be applied to characterize the optical properties of nanotriangles without loss of generality. In the present work, the polarization vector **E** is always parallel to the triangular cross section. The refractive index of the surrounding media is set as 1.33. The properties of nanotriangles are the same as last section. Only the extinction efficiency is shown to evaluate the optical properties of gold nanotriangular prism since the scattering efficiency is too small compared to the absorption efficiency. All cases are implemented using the DDSCAT 7.3 package, and it is executed on an Intel Core i7-3770 PC with 8GB RAM.

### 3.1. Influence of aspect ratio

The aspect ratio is a crucial factor which has an influence on the optical properties of asymmetrical nanoparticles. The extinc-
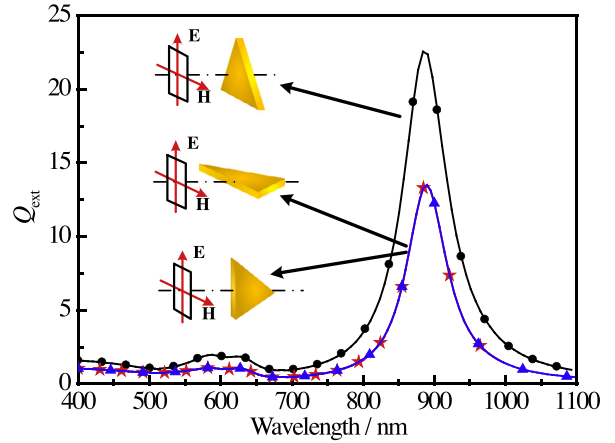


**Fig. 2.** Extinction efficiency for an individual gold nanotriangle at different incident angles. Side length of the triangle is 80 nm and height is 8 nm.

tion efficiency of nanotriangular prisms for different lengths and the same height are shown in Fig. 3. The height is set as 8 nm and the length ranges from 20 nm to 200 nm. It can be seen that there is more than one peak in the spectral extinction efficiency for larger nanotriangles, which is caused by multipolar plasmon extinction [20]. The multipolar plasmon extinction is induced by the inhomogeneity of the electromagnetic field [23]. Usually, higher order of plasmon resonance can be excited for larger nanoparticles. Obviously, there is a redshift of the 1st order resonance with the increasing of edge length ($l$ represents the multipolar order in Fig. 3). Since the higher order resonance ($l > 1$) is relatively weak, for smaller particles they can be submerged by the dominated 1st order resonance. Furthermore, it can be seen that there is a wide and tunable range for the peak extinction, which is a favorable characteristic for the application of nanoparticle based therapeutic and diagnostic approaches. It also can be seen from Fig. 3(b) that the higher order ($l = 2$ and 3) resonances are well resolved from the lower order resonances, when the effective radius of the media is larger than a critical value. This make it possible to investigate each resonance band in the context of nanoscale applications. These spectral features could be very promising in nanooptics or for chemosensing and biosensing applications [20].

It is interesting that well-defined trends of the extinction spectra maxima for multipolar plasmon extinction ($l = 1$, 2, and 3) are observed. There is a linear correlation between the resonance wavelength and edge length (see Fig. 4). It can be seen that the tunable wavelength of the 1st order resonance (black square) covers a relatively large interval which is from visible to near-infrared, which is a distinct advantage in the application of nanomedicine. Furthermore, it is more sensitive to edge length than the 2nd (blue triangle) and 3rd (red circle) order resonances, since it has a larger slope. Meanwhile, the 2nd and 3rd order resonances wavelength is basically in the visible region.

### 3.2. Interaction of two nanotriangles aligned side-by-side

The near-field interaction between nanoparticles may have significant effect on their optical properties. In this section, the extinction efficiency of nanotriangles dimer aligned side-by-side (see inset of Fig. 5a) was studied. The scanning electron microscopy image of nanotriangle dimers can be found in other references [28,30]. The polarization vector **E** is parallel to the triangle prism cross section and perpendicular to one side of the triangle. The side length of the triangle is set as $L = 60$ and 120 nm (see Fig. 5a and b), and the height of the prism is $H = 8$ nm.

Compared to an individual nanotriangle, there are four peaks in the extinction spectra instead of three ($l = 1$, 2, and 3). The posi-
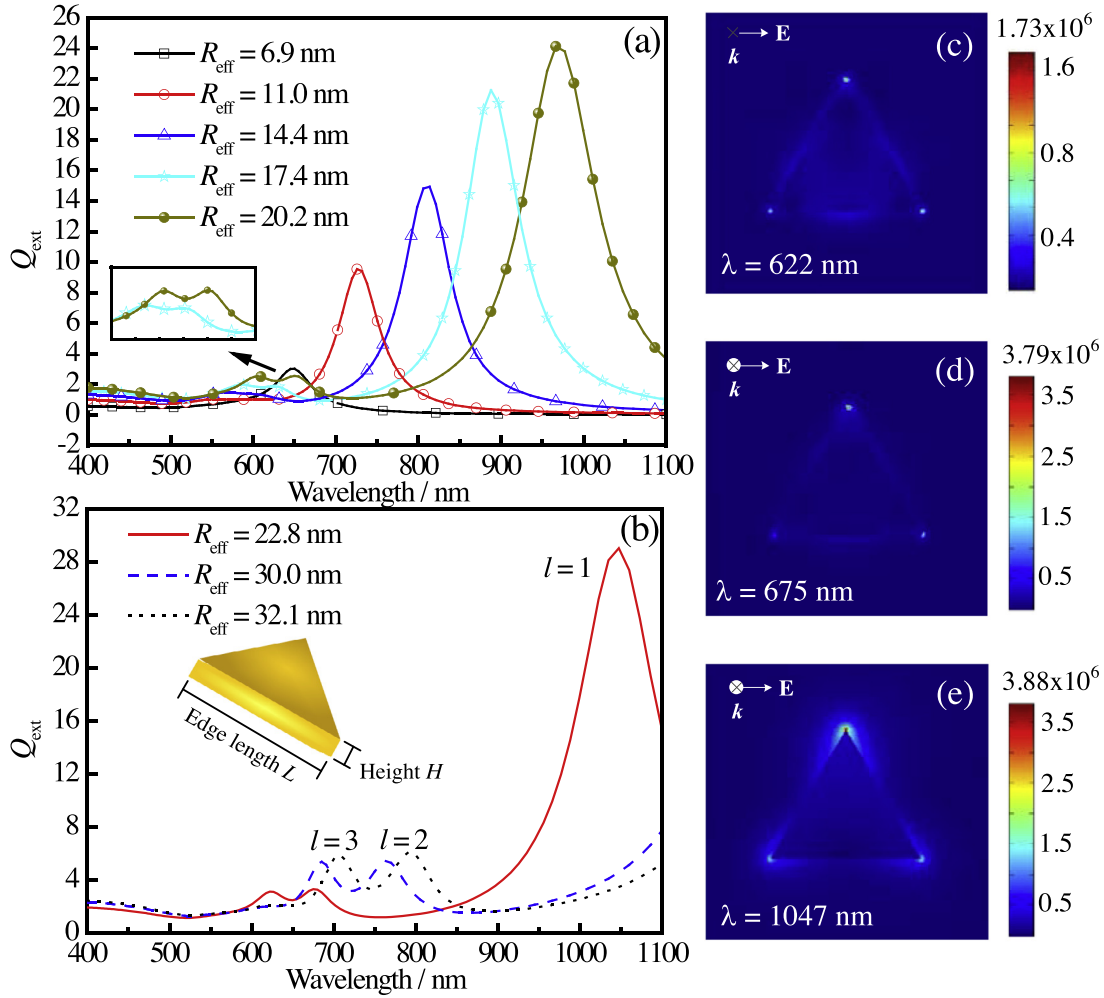
**Fig. 3.** Calculated extinction efficiency of nanotriangular prism with different edge lengths ($L = 20$, 40, 60, 80, 100, 120, 180, and 200 nm) and same height ($H = 8$ nm), corresponding to (a) $R_{eff} = 6.9$, 11.0, 14.4, 17.4, and 20.2 nm; (b) 22.8, 30.0 and 32.1 nm; (c), (d), and (e) electric field of nanotriangle with $R_{eff} = 22.8$ nm.
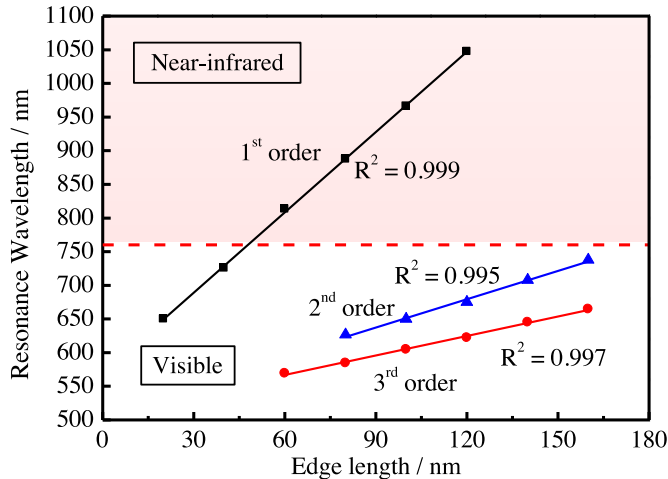


**Fig. 4.** Linear fitting of the resonance wavelength and edge length for nanotriangles with $H = 8$ nm.

tions of peaks corresponding to $l = 2$ and 3 are influenced by the offset distance. However, a fourth peak arises in the long wave band, which is induced by the interaction between two particles. With the increasing of offset distance $s$, the interaction is weakened and a blue shift of the fourth peak is observed. When $s$ is larger than a critical value, the two peaks merge together, which

results in a slightly red shift of the 1st order resonance. It is interesting to note that, when $s > L$, the fourth peak will vanish and the resonance wavelength will equal to that of one single nanotriangle (black dashed lines in Fig. 5). Furthermore, when the distance $s$ is relatively small, a shoulder (red dashed circle in Fig. 5) becomes conscious of in the blue side of the peak, which corresponds to the out-of-plane mode.

The wavelength of peak extinction $\lambda_{max}$ with respect to the ratio of offset distance $s$ and edge length $L$ is shown in Fig. 6. For the third peak ($l = 1$), $\lambda_{max}$ is almost a constant which is independent of distance $s$. Meanwhile, this constant is very close to the resonance wavelength of an individual nanotriangle (see black dashed lines in Fig. 6), which means that this peak corresponds to the in-plane mode. The small offset of the $\lambda_{max}$ from the solid line is caused by the effect of the fourth peak, which is induced by the interaction between the two particles. When $s$ is large, the interaction is too weak to make a difference on the extinction spectra. However, when $s$ is small, an additional peak is generated and it appears to have an exponential relationship with the ratio of offset distance $s$ and edge length $L$ (see Fig. 6), which can be expressed as:

$$\frac{\Delta\lambda}{\lambda_{max}} = a\exp\left(-\frac{s/L}{b}\right) \qquad (7)$$

where $\lambda_{max}$ is the additional peak position. $\Delta\lambda$ is the red shift of $\lambda_{max}$ compared to individual nanotriangle. The red shift phenomenon is similar to that of the nanorod dimer [26], which also
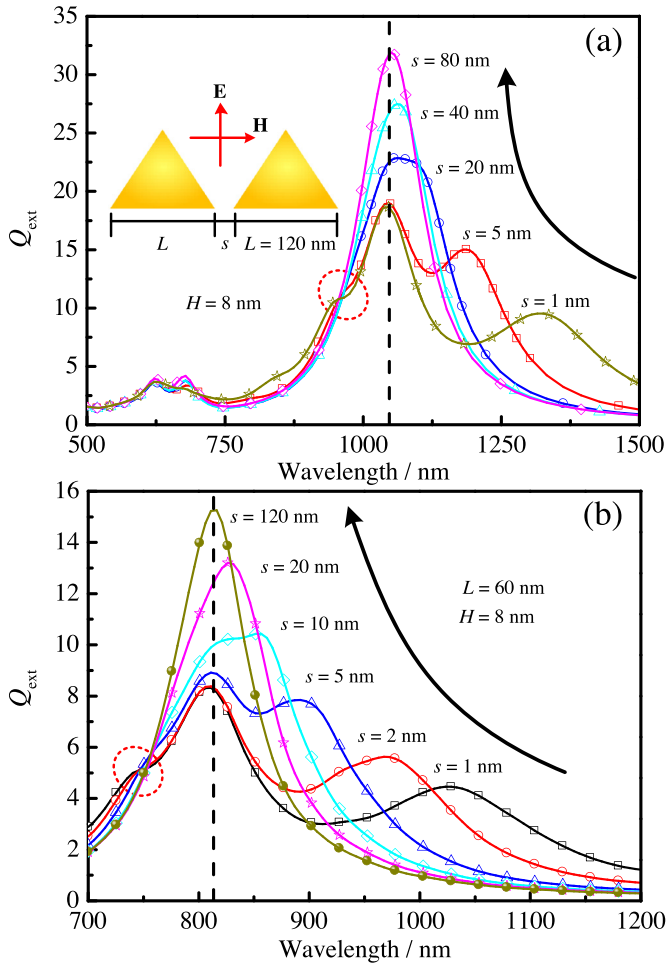
**Fig. 5.** Extinction efficiency of two nanotriangles aligned side-by-side in different distances. (a) $L = 120$ nm and $H = 8$ nm; (b) $L = 60$ nm and $H = 8$ nm. The black dashed lines refer to the resonance position of an individual nanotriangle with the same size.
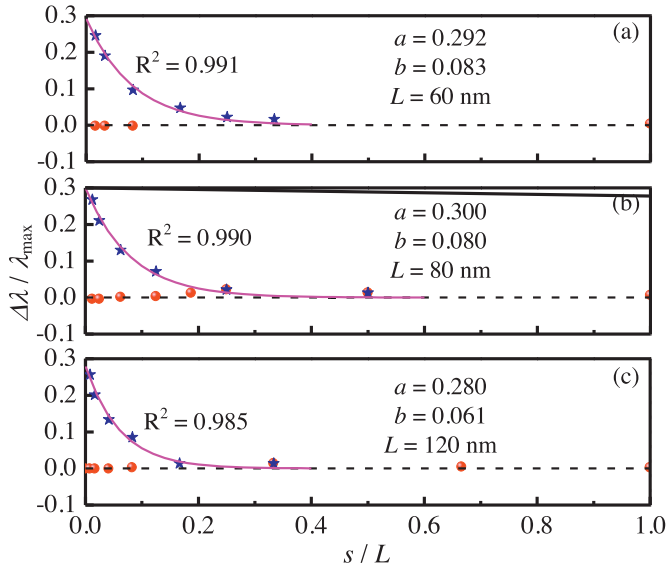


**Fig. 6.** Resonance wavelength for nanotriangle dimers with (a) $L = 60$ nm; (b) $L = 80$ nm; and (c) $L = 120$ nm. The red spheres represent the resonance wavelength correspond to $l = 1$. Black dashed lines are the peak position for an individual nanotriangle with the same size. Blue stars are the peak positions of the additional peaks which can be fitted using Eq. (7) (solid lines). (For interpretation of the references to color in this figure legend, the reader is referred to the web version of this article.)
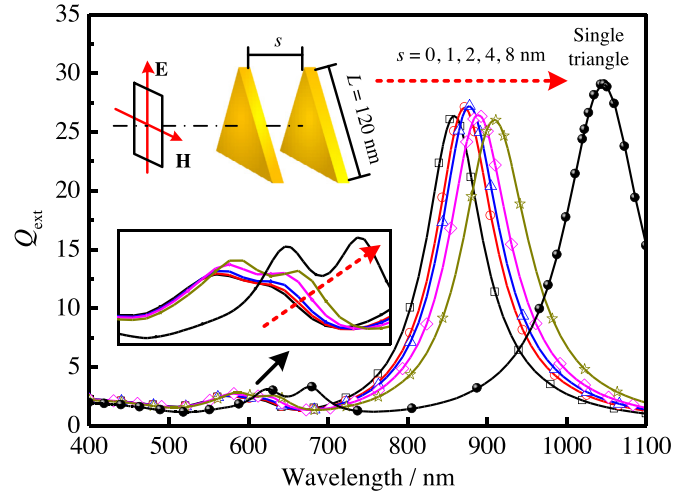


**Fig. 7.** Extinction efficiency of nanotriangle dimers with triangles placed parallel along the prism axis.

can be expressed as an exponential relation. However, for the nanorod, there will not be an additional peak. For nanotriangles dimers, when $s/L$ is larger than 0.3, the peak position has almost no difference with that of an individual triangular prism.

### 3.3. Interaction of two nanotriangles arranged in line

Compared to side-by-side arrangement, the dimer structure with triangles placed parallel along the prism axis has a relatively small influence on the extinction spectra. Only a blue shift of the resonance peak ($l = 1$, 2, and 3) is observed. It almost does not change the pattern of the extinction efficiency when the polarization vector **E** is parallel to the triangle prism cross section and perpendicular to one side of the triangle (see Fig. 7). The side length of the triangle is set as $L = 120$ nm and the height of the prism is $H = 8$ nm. Different from the side by side dimer structure, the offset distance $s$ also has an influence on the higher order resonance ($l = 2$ and 3), which is because $l = 2$ and 3 are out-of-plane resonance which is also along the prism axis direction. The adjoining of another particle in that direction will certainly affect the resonance wavelength and amplitude. With the increasing of the offset distance, the interaction between two particles becomes so weak that the extinction spectra will be the same single nanotriangle problem.

### 3.4. Interaction of two nanotriangles aligned bottom-to-bottom

In this section, another type of nanotriangle dimer was investigated. The two nanotriangles are placed bottom-to-bottom. The polarization vector **E** is parallel to the triangle prism cross section and perpendicular to parallel side of the triangles (see inset of Fig. 8). As can be seen from Fig. 8, when the offset distance is larger than a critical value, the resonance wavelength will coincide with that of an individual nanotriangle which is similar to the other two conditions mentioned above. It is interesting to note that with the decreasing of $s$, the resonance peak correspond to in-plane mode splits into two. This phenomenon also can be observed in other kinds of nanoparticle dimers, such as nanocube [53] and nanorod [26]. This is caused by the enhancement of local electromagnetic field, which is why the resonance peak position is related to the distance between the two nanotriangles. The red shift side (right side) has a red shift trend and the blue shift side (left side) has a blue shift trend when continuously decrease $s$. $s = 0$ is equivalent to the condition of a rhombus. Moreover, the wavelength of
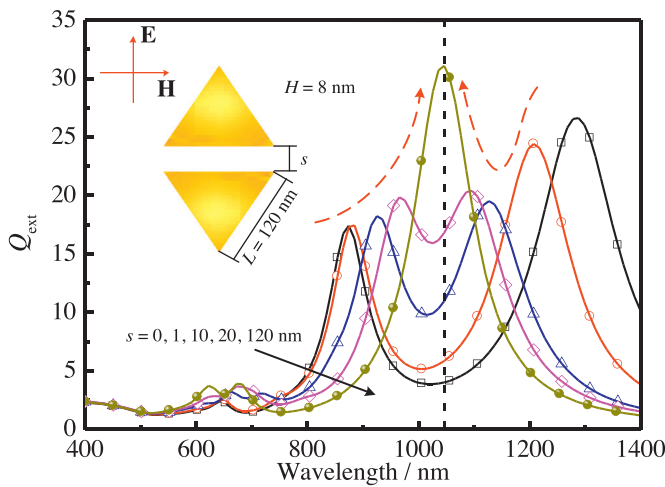
**Fig. 8.** Extinction efficiency of two nanotriangles aligned bottom-to-bottom.
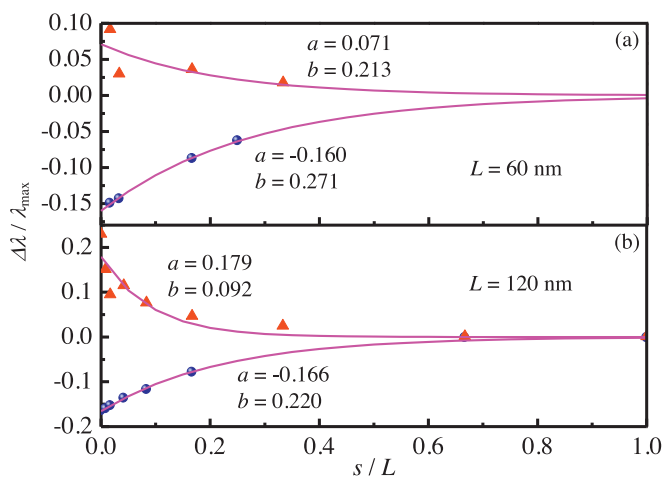


**Fig. 9.** Resonance wavelength for nanotriangle dimers with (a) $L = 60$ nm and (b) $L = 120$ nm for different apart distances. The red triangle and blue spheres represent the resonance wavelength on the red and blue sides of the peak corresponding to an individual nanotriangle, respectively. Solid lines are the fitted data using Eq. (7). (For interpretation of the references to color in this figure legend, the reader is referred to the web version of this article.)

peak extinction $\lambda_{max}$ also can be fitted as an exponential correlation (see Eq. (7)) with the ratio of offset distance $s$ and edge length $L$ (see Fig. 9).

## 4. Conclusions

In the present work, a promising type of gold nanoparticle, triangular prism was under investigation. The DDSCAT package was employed to study the optical properties of an individual nanotriangular prism and triangular dimers, including two nanotriangles aligned side-by-side, bottom-to-bottom, and in line. The influence of different size and offset distance were considered, which could be meaningful for the applications in variety fields, such as surface-enhanced Raman spectroscopy, universal plasmon ruler, and optoelectronic field. Theoretical studies on the optical properties of gold nanotriangle dimers are present to show how relative positions affect the extinction spectra. Main conclusions can be drawn as follows:

(1) Well-defined trends of the extinction spectra maxima for lower order extinction, which correspond to in-plane mode, were observed, which has a linear correlation with the triangle edge length.

(2) For the side-by-side arrangement, an additional peak was generated on the red shift side of the peak correspond to dipole mode. When the distance between two prisms was scaled by the triangular side length, the relative plasmon shift can be approximated to an exponential relation with the relative offset distance.

(3) For dimers with nanotriangles arranged in line, there was a global blue shift of the extinction spectra with the approaching of two particles.

(4) For dimers with two nanotriangles aligned bottom-to-bottom, the resonance band split into two bands with the decreasing of the offset distance.

Further studies will be focused on the interaction of three or more nanoparticles.

## References

[1] Chen G, Roy I, Yang C, Prasad PN. Nanochemistry and nanomedicine for nanoparticle-based diagnostics and therapy. Chem Rev 2016;116:2826–86.
[2] Pang B, Yang X, Xia Y. Putting gold nanocages to work for optical imaging, controlled release and cancer theranostics. Nanomedicine 2016;11:1715–28.
[3] Dombrovsky LA, Timchenko V, Jackson M, Yeoh GH. A combined transient thermal model for laser hyperthermia of tumors with embedded gold nanoshells. Int J Heat Mass Transfer 2011;54:5459–69.
[4] Khlebtsov NG, Dykman LA. Optical properties and biomedical applications of plasmonic nanoparticles. J Quant Spectrosc Radiat Transfer 2010;111:1–35.
[5] Zhang LD, Chen X, Wu YT, Lu YW, Ma CF. Effect of nanoparticle dispersion on enhancing the specific heat capacity of quaternary nitrate for solar thermal energy storage application. Sol Energy Mater Sol Cells 2016;157:808–13.
[6] Chen M, He Y, Zhu J, Shuai Y, Jiang B, Huang Y. An experimental investigation on sunlight absorption characteristics of silver nanofluids. Sol Energy 2015;115:85–94.
[7] Saha K, Agasti SS, Kim C, Li X, Rotello VM. Gold nanoparticles in chemical and biological sensing. Chem Rev 2012;112:2739–79.
[8] Salata O. Applications of nanoparticles in biology and medicine. J Nanobiotechnol 2004;2:1–6.
[9] Zakomirnyi VI, Rasskazov IL, Karpov SV, Polyutov SP. New ideally absorbing Au plasmonic nanostructures for biomedical applications. J Quant Spectrosc Radiat Transfer 2016.
[10] Xia Y, Gilroy KD, Peng HC, Xia X. Seed-mediated growth of colloidal metal nanocrystals. Angew Chem Int Ed 2017;56:60–95.
[11] Onofri FRA, Barbosa S, Touré O, Woźniak M, Grisolia C. Sizing highly-ordered buckyball-shaped aggregates of colloidal nanoparticles by light extinction spectroscopy. J Quant Spectrosc Radiat Transfer 2013;126:160–8.
[12] Falamas A, Tosa N, Tosa V. Dynamics of laser excited colloidal gold nanoparticles functionalized with cysteine derivatives. J Quant Spectrosc Radiat Transfer 2015;162:207–12.
[13] Dombrovsky LA, Timchenko V, Jackson M. Indirect heating strategy for laser induced hyperthermia: an advanced thermal model. Int J Heat Mass Transfer 2012;55:4688–700.
[14] Albanese A, Chan WC. Effect of gold nanoparticle aggregation on cell uptake and toxicity. ACS Nano 2011;5:5478–89.
[15] Ghosh P, Han G, De M, Kim CK, Rotello VM. Gold nanoparticles in delivery applications. Adv Drug Delivery Rev 2008;60:1307–15.
[16] Ren Y, Qi H, Chen Q, Ruan L. Thermal dosage investigation for optimal temperature distribution in gold nanoparticle enhanced photothermal therapy. Int J Heat Mass Transfer 2017;106:212–21.
[17] Huang X, El-Sayed MA. Gold nanoparticles: Optical properties and implementations in cancer diagnosis and photothermal therapy. J Adv Res 2010;1:13–28.
[18] Myroshnychenko V, Rodríguez-Fernández J, Pastoriza-Santos I, Funston AM, Novo C, Mulvaney P, et al. Modelling the optical response of gold nanoparticles. Chem Soc Rev 2008;37:1792–805.
[19] Rai Akhilesh, Singh Amit, Absar Ahmad A, Sastry M. Role of halide ions and temperature on the morphology of biologically synthesized gold nanotriangles. Langmuir 2006;22:736–41.

[20] Félidj N, Grand J, Laurent G, Aubard J, Lévi G, Hohenau A, et al. Multipolar surface plasmon peaks on gold nanotriangles. J Chem Phys 2008;128:094702.

[21] Shuford KL, Ratner MA, Schatz GC. Multipolar excitation in triangular nanoprisms. J Chem Phys 2005;123:830–45.

[22] Krenn JR, Schider G, Rechberger W, Lamprecht B. Design of multipolar plasmon excitations in silver nanoparticles. Appl Phys Lett 2000;77:3379–81.

[23] Laurent G, Félidj N, Aubard J, Lévi G, Krenn JR, Hohenau A, et al. Surface enhanced Raman scattering arising from multipolar plasmon excitation. J Chem Phys 2005;122:119–90.

[24] Cuevas M, Riso MA, Depine RA. Complex frequencies and field distributions of localized surface plasmon modes in graphene-coated subwavelength wires. J Quant Spectrosc Radiat Transfer 2016;173:26–33.

[25] Didari A, Mengüç MP. Near-field thermal emission between corrugated surfaces separated by nano-gaps. J Quant Spectrosc Radiat Transfer 2015;158:43–51.

[26] Funston AM, Novo C, Davis TJ, Mulvaney P. Plasmon coupling of gold nanorods at short distances and in different geometries. Nano Lett 2009;9:1651–8.

[27] Humphrey A, Barnes W. Plasmonic surface lattice resonances in arrays of metallic nanoparticle dimers. J Optics 2016;18:035005.

[28] Lin TR, Chang SW, Chuang SL, Zhang Z, Schuck PJ. Coating effect on optical resonance of plasmonic nanobowtie antenna. Appl Phys Lett 2010;97 063106–3.

[29] Grześkiewicz B, Ptaszyński K, Kotkowiak M. Near and far-field properties of nanoprisms with rounded edges. Plasmonics 2014;9:607–14.

[30] Rosen DA, Tao AR. Modeling the optical properties of bowtie antenna generated by self-assembled Ag triangular nanoprisms. Acs Appl Mater Interfaces 2014;6:4134–42.

[31] Zhang C, Zhu J, Li J, Zhao J. Misalign-dependent double plasmon modes "switch" of gold triangular nanoplate dimers. J Appl Phys 2015;117:063102.

[32] Kotkowiak M, Grześkiewicz B, Robak E, Wolarz E. Interaction between nanoprisms with different coupling strength. J Phys Chem C 2015;119.

[33] Azarian A, Babaei F. Localized surface plasmons in face to face dimer silver triangular prism nanoparticles. J Appl Phys 2016;119:203103.

[34] Hodkinson J, Greenleaves I. Computations of light-scattering and extinction by spheres according to diffraction and geometrical optics, and some comparisons with the Mie theory. J Opt Soc Am A 1963;53:577–88.

[35] Flatau PJ, Draine BT. Fast near field calculations in the discrete dipole approximation for regular rectilinear grids. Opt Express 2012;20:1247–52.

[36] Edalatpour S, Francoeur M. The Thermal Discrete Dipole Approximation (T-DDA) for near-field radiative heat transfer simulations in three-dimensional arbitrary geometries. J Quant Spectrosc Radiat Transfer 2014;133:364–73.

[37] Lee K-S, El-Sayed MA. Dependence of the enhanced optical scattering efficiency relative to that of absorption for gold metal nanorods on aspect ratio, size, end-cap shape, and medium refractive index. J Phys Chem B 2005;109:20331–8.

[38] Weber-Bargioni A, Schwartzberg A, Schmidt M, Harteneck B, Ogletree DF, Schuck PJ, et al. Functional plasmonic antenna scanning probes fabricated by induced-deposition mask lithography. Nanotechnology 2010;21:065306.

[39] Jiang J, Krauss TD, Brus LE. Electrostatic force microscopy characterization of trioctylphosphine oxide self-assembled monolayers on graphite. J Phys Chem B 2000;104:11936–41.

[40] Huang W, Qian W, Jain PK, El-sayed MA. The effect of plasmon field on the coherent lattice phonon oscillation in electron-beam Fabricated gold nanoparticle pairs. Nano Lett 2007;7:3227–34.

[41] Takahashi S, Zayats AV. Near-field second-harmonic generation at a metal tip apex. Appl Phys Lett 2002;80:3479–81.

[42] Zhang Z, Weberbargioni A, Wu SW, Dhuey S, Cabrini S, Schuck PJ. Manipulating nanoscale light fields with the asymmetric bowtie nano-colorsorter. Nano Lett 2010;9:4505.

[43] Brongersma ML. Plasmonics: electromagnetic energy transfer and switching in nanoparticle chain-arrays below the diffraction limit. Phys Rev B 2000;62:16356–9.

[44] Maier SA, Kik PG, Atwater HA. Observation of coupled plasmon-polariton modes in Au nanoparticle chain waveguides of different lengths: estimation of waveguide loss. Appl Phys Lett 2002;81:1714–16.

[45] Reinhard BM, Siu M, Agarwal H, Alivisatos AP, Liphardt J. Calibration of dynamic molecular rulers based on plasmon coupling between gold nanoparticles. 2005;5:2246–52.

[46] Reinhard BM, Sheikholeslami S, Mastroianni A, Alivisatos AP, Liphardt J. Use of plasmon coupling to reveal the dynamics of DNA bending and cleavage by single ecorv restriction enzymes. Proc Natl Acad Sci USA 2007;104:2667–72.

[47] Krenn JR, Dereux A, Weeber JC, Bourillot E, Lacroute Y, Goudonnet JP, et al. Squeezing the optical near-field zone by plasmon coupling of metallic nanoparticles. Phys Rev Lett 1999;82:2590.

[48] Draine BT, Flatau PJ. Discrete-dipole approximation for scattering calculations. J Opt Soc Am A 1994;11:1491–9.

[49] Draine BT. Discrete-dipole approximation and its application to interstellar graphite grains. Astrophys J 1988;333:848–72.

[50] Flatau PJ. Improvements of the discrete dipole approximation method. Opt Lett 2000;22:1205–7.

[51] Jain PK, Lee KS, El-Sayed IH, El-Sayed MA. Calculated absorption and scattering properties of gold nanoparticles of different size, shape, and composition: applications in biological imaging and biomedicine. J Phys Chem B 2006;110:7238–48.

[52] Johnson PB. Optical constants of the noble metals. Phys Rev B 1972;6:4370–9.

[53] Hooshmand N, Bordley JA, Elsayed MA. Plasmonic spectroscopy: the electromagnetic field strength and its distribution determine the sensitivity factor of face-to-face Ag nanocube dimers in solution and on a substrate. J Phys Chem C 2015;119:15579–87.